Hydrogen fuel cell integration and testing in a hybrid-electric propulsion rig

João Farinha, Luís Miguel Silva, Jay Matlock, Frederico Afonso, & Afzal Suleman

2023

Available online at www.sciencedirect.com

ScienceDirect

journal homepage: www.elsevier.com/locate/he

Hydrogen fuel cell integration and testing in a hybrid-electric propulsion rig

João Farinha [a,b], Luís Miguel Silva [a,b], Jay Matlock [b], Frederico Afonso [a], Afzal Suleman [a,b,*]

[a] Universidade de Lisboa, Instituto Superior Técnico, IDMEC, Lisbon, Portugal
[b] University of Victoria, Centre for Aerospace Research, Victoria, British Columbia, Canada

HIGHLIGHTS

- A parallel hybrid architecture using batteries and fuel cells was tested.
- Splitting power from one side to the other may lessen fuel requirements.
- The fuel cell performance was found to depend greatly on the testing conditions.

GRAPHICAL ABSTRACT

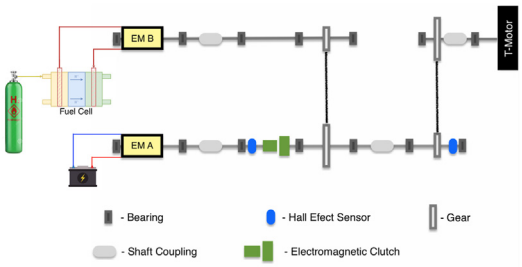

ARTICLE INFO

Article history:
Received 2 April 2023
Received in revised form
31 May 2023
Accepted 8 June 2023
Available online xxx

Keywords:
Hybrid-electric propulsion
Parallel configuration
Hydrogen fuel cell
Unmanned aerial vehicle

ABSTRACT

On the road towards greener aviation, hybrid-electric propulsion systems have emerged as a viable solution. In this paper, a system based on hydrogen fuel cells is proposed and evaluated in a laboratory setting with its future integration in a propulsive system in mind and main focus on the ability to lessen the power demand on the opposing side of the bench. The setup consists in a parallel architecture with two power sources: a hydrogen fuel cell and a battery. First, the performance of the fuel cell and its capability to provide power to one of the motors are analyzed. Then, the entire parallel hybrid system is evaluated. Although the experimental setup was shown to be sub-optimal, the results demonstrated the ability of this greener alternative to reduce power demand on the opposing side of the parallel configuration, with a reduction of up to 40.3% in the highest load scenario, and maximum power output on the fuel cell of 257.8 W. The stack performance was also concluded to be very dependent on the operating temperature.

* *Corresponding author*. Universidade de Lisboa, Instituto Superior Técnico, IDMEC, Lisbon, Portugal.
E-mail address: suleman@tecnico.ulisboa.pt (A. Suleman).

https://doi.org/10.1016/j.ijhydene.2023.06.090

Introduction

As the years pass, climate change and greenhouse gases emissions increasingly become a more pressing issue. As public awareness towards the issue grows, and policies shift to more environmentally friendly ones, the industrial world has to adapt. The aviation industry is no exception in this need for change, and hybrid electric propulsion appears as part of the solution for this sector.

The largest known impact of aviation on the environment comes from atmospheric emissions of pollutant gases, in particular carbon dioxide (CO_2) and nitrogen oxides (NO_x), although more recently aircraft-induced clouds are also being pointed out as relevant focus of concern [1]. Carbon dioxide emissions are one of the main source for human-made climate change, and the aviation sector contributes significantly to emissions. By 1992 this sector already represented 2% of human emissions of this gas [2]. By 2010 it was the source of at least 3% of the total anthropogenic CO_2 emissions, showing a growth trend [3]. NO_x on the other hand is a pollutant that triggered the production of ozone, especially at the typical cruise altitude for modern aircraft [4]. Pollution emissions, besides their climate impact, also constitute a health hazard [5]. An estimated 16 thousand premature deaths are caused annually. These can be mainly attributed to fine particles, $PM_{2.5}$, emitted during aircraft operation [6].

With the goal of reducing emissions and saving fuel, hybrid electric propulsion systems constitute an attractive option being studied for eventual implementation in large-scale aircraft. However, the viability of such solutions requires overcoming several obstacles, such as energy storage and thermal management [7–9]. A hybrid electric propulsion system (HEPS) refers to a system that draws power from two (or, potentially, more) different energy sources to generate the propulsive force for the aircraft, and at least one of them generates electrical power [10]. The objective is to combine the strengths of different types of propulsive systems, while minimizing their drawbacks.

In the context of hybrid propulsion research, one particular energy source that seems to have a lot of potential is hydrogen [11], including for aviation [12]. This gas has a very high energy density, which makes it attractive as an alternative to fossil fuels since a small weight of hydrogen can store a lot of energy, an important aspect for aerospace applications. Being flammable, and very reactive, it can be burned directly with oxygen, or used in a fuel cell (FC) to produce electricity [13]. This presents an alternative to traditional batteries for electricity-powered vehicles. This type of energy source comes across as a more environmentally friendly substitute for fossil fuels [14], as the product of the reaction with oxygen is just water, and hydrogen can be produced renewably from water as well. However, this type of energy source also present several challenges to its widespread implementation [15]. Its low volumetric energy density in the gaseous state presents issues when it comes to onboard storage solutions. Another issue associated to FCs is their short lifetime caused by degradation [16]. Besides, the production of renewable hydrogen is not yet economically competitive despite technically feasible [17]. These issues will need to be addressed for a successful utilization of this fuel in aviation, and justify the importance of further studying these technologies [18].

Before its application in large aircraft, hydrogen-based propulsion systems have to be further studied, starting with test bench tests, and small Unmanned Aerial Vehicle (UAV) applications, to minimize risks and cost. Some early examples of UAVs powered by FCs, using different storage solutions, include the one tested by Bradley et al. [19], with a 500 W FC and compressed hydrogen storage, and the one designed by Kim et al. [20], using a hydrid to power a 100 W FC. As this topic remains of interest, several authors [21–24] have tested different concepts consisting mainly in parallel hybrid layouts combining Lithium-Polymer (Li–Po) batteries and a proton exchange membrane fuel cell (PEMFC). A suitable energy management system is required to deal with the different power rates encountered in flight which can reduce hybrid system performance [25]. This can be done for instance through controlling DC/DC converters associated to the FC [25,26], and using fuzzy logic [21] or maximum power point tracking [27,28]. Further efficiency benefits can be found by combing an energy management system with trajectory control [24]. There are also efforts on developing hybrid systems with solid oxide fuel cell (SOFC) at the computational level considering engines [29–31], thermoelectric generators [32], and combining thermionic and thermoelectric generators [33]. Several test bench experiments have been conducted on hybrid systems using PEMFCs to augment UAV capacity [21–24,34]. A different concept was successfully flight tested by Boeing onboard of a small UAV, whose hybrid propulsion system runs on hydrides that fed a generator which provides hydrogen to a FC [35].

In this work, a hydrogen FC has been integrated as a power source in a parallel hybrid configuration, to study its viability as an energy source for UAVs. This development follows a series of experiments performed on the FC on its own, as well as a series of projects focused on studying parallel hybrid-electric configuration [36]. This article distinguishes itself from the previously presented works in the literature by the uniqueness of its experimental setup architecture: the mechanical coupling of these two power sources (battery and hydrogen fuel cell) in a parallel hybrid configuration, together with the adjustable dynamometer setup at the output shaft. This combination constitutes an unexplored approach, to the best of our knowledge.

This paper begins with a brief review of FC technology and parallel hybrid systems, in this section; then, section Experimental Setup describes the fuel cell system used and the test bed for the experiments; section Test Procedure summarizes the test procedure; section Results presents the main results collected and their analysis; and finally, the conclusions are in section Conclusions.

Technology overview

Fuel cell technology

Fuel cells are electrochemical devices that produce continuous electric power, generated through a chemical reaction. They are open systems, needing a constant input of fuel and oxidizer to generate power, working as power sources, as long

Please cite this article as: Farinha J et al., Hydrogen fuel cell integration and testing in a hybrid-electric propulsion rig, International Journal of Hydrogen Energy, https://doi.org/10.1016/j.ijhydene.2023.06.090

as there is fuel and oxidizer flow. While both batteries and fuel cells generate direct current, the specific energy of FCs is considerably larger than that of batteries, given hydrogen's high energy density [37].

There are several different types of fuel cells, such as PEMFC, SOFC, and direct methanol fuel cell (DMFC). The one used in this work was a PEMFC.

The PEMFC is essentially made up of three parts: anode, cathode, and the proton exchange membrane, or PEM, located in between the two sides. This central membrane allows for protons (H^+) to pass from one side to the other [38]. Each electrode has a porous diffusion layer and a catalyst layer, to facilitate the chemical reactions in both the anode and cathode [39]. The reactions in the anode and the cathode can be written, respectively, as

$$H_2 \rightarrow 2H^+ + 2e^-, \quad (1)$$

and

$$\frac{1}{2}O_2 + 2H^+ + 2e^- \rightarrow H_2O, \quad (2)$$

with the overall reaction being simply

$$\frac{1}{2}O_2 + H_2 \rightarrow H_2O. \quad (3)$$

The two protons created on the anode move to the cathode through the PEM, as mentioned, while the free electrons movement correspond to the electric current. A schematic representation of the PEMFC working principle is depicted in Fig. 1.

Currently, this type of fuel cell is the most used in UAV applications [40]. The main advantage PEMFC has over other possibilities lies with its low operating temperature (from 30 °C to 110 °C [40]), when compared to other types of FC, such as SOFC [41]. Nevertheless, such a FC still needs a thermal management system to improve its operational efficiency and safety [42]. Besides, they are also small, and present comparatively high operating efficiency (40 ~60%) [40]. However, the main issue faced by this type of FC is the high cost. Both the PEM and the catalyst necessary are expensive [43]. Moreover, the storage of hydrogen can be a problem, given its low density, requiring large and heavy containers, if stored in gaseous form [44].

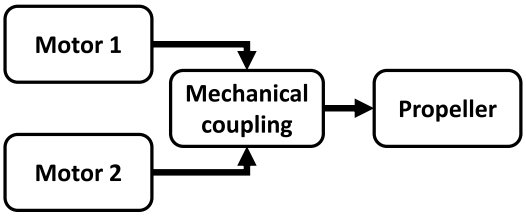

Fig. 2 – Parallel hybrid configuration.

Parallel hybrid systems

In a hybrid electric propulsion system using a parallel configuration, like the one depicted schematically in Fig. 2, an electric motor and an engine/motor are mechanically coupled, allowing for both to drive the propeller at the same time, with their torque being added by the coupling [45]. It can include one or more clutches, to disconnect one of the power sources, in case it is not being used.

The mechanical transmission in this configuration is more complex, when compared to a series configuration, and the controller design is not as simple. However, this architecture can provide mass savings for the system. As the maximum power can be achieved by combining both motors, they can be downsized. The possibility of both power sources to drive the propeller independently also offers some redundancy to the system [45].

In a parallel hybrid system, several distinct operating modes can be defined. The system can have a single power source driving the propeller at a time, while the other is turned off. In case a clutch is present, the side not being used may be completely disconnected from the system, otherwise,

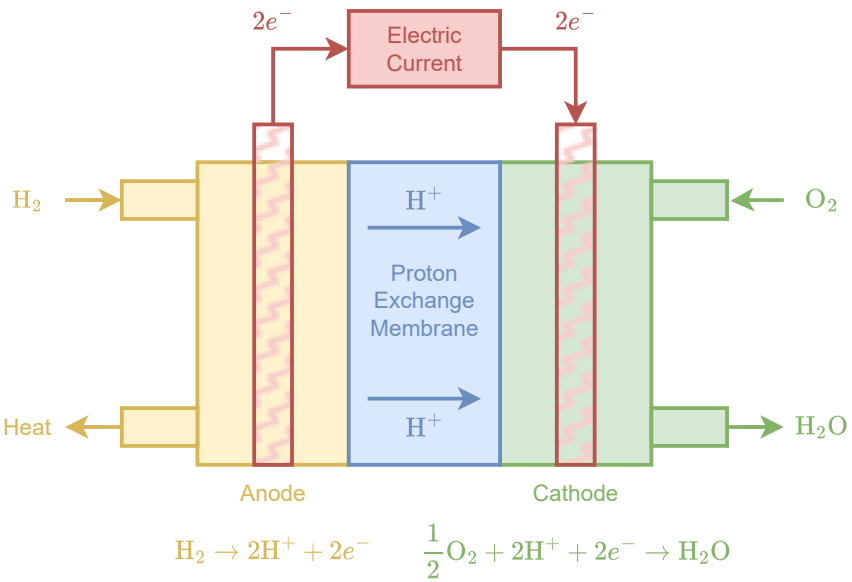

Fig. 1 – PEMFC representation, based on [18].

Please cite this article as: Farinha J et al., Hydrogen fuel cell integration and testing in a hybrid-electric propulsion rig, International Journal of Hydrogen Energy, https://doi.org/10.1016/j.ijhydene.2023.06.090

additional power will be consumed to rotate the inactive side [45]. Alternatively, during hybrid/dash operation, both energy sources are combined, to achieve additional power. This mode has to be sized to fulfill the power requirements of the most demanding flight phases, such as take-off and climb. Finally, a regeneration mode can also be defined for a generic parallel hybrid system. This takes advantage of both sides of the system, but this time using one of them to charge the system's batteries on the other. This is made possible by using an electric motor as a generator [45].

Experimental setup

The experimental setup used consisted essentially of two subsystems: the hydrogen FC system, and the hybrid propulsion test bench, shown in Figs. 3 and 4, respectively.

Fuel cell system

The HP 600 fuel cell system (Fig. 3) is an experimental module designed for educational and research purposes, distributed by Heliocentris Energy Systems GmbH [46]. Its core component is the BZ 130 FC stack, produced by Ulmer Brennstoffzellen-Manufaktur GmbH (UBzM). The stack is composed of 24 PEM fuel cells, each with 126 cm^2 of area, and it is rated for a power of 600 W, has an open circuit voltage of 23.5 V, and a maximum current of 45 A. Its recommended operating temperatures are between 45 °C and 60 °C. The system has two operating modes: unregulated, where the load is directly connected to the FC stack, and regulated, in which the fuel cell power passes through a DC/DC converter to ensure constant output voltage.

The cathode of the stack uses oxygen from atmospheric air, which passes through a filter prior to entering the system, and through a fan that adjusts the amount of air intake. Besides the air entrance, the humid air exhaust is also adjusted by the system, according to the temperature and humidity in the cathode air channel. This creates an air recirculation channel, allowing for the system's membrane to be self-humidified by the air in the cathode. The anode requires hydrogen at a purity grade of at least 5.0 (99.999%), which came from an external compressed gas cylinder, Praxair's Ultra High Purity 5.0 Hydrogen Cylinder (Fig. 3b). This cylinder stored hydrogen at a maximum pressure of 165.5 bar. To be used, its pressure had to be reduced to between 2 and 17 bar, as per the manufacturer's indications, using an appropriate regulator, in this case a Harris KH1130, also visible in Fig. 3b. On the left side of the FC stack there is the exhaust air outlet, where the water generated during the hydrogen oxidation process in the cathode can leave the system as moisture.

Besides the stack, the system includes several auxiliary systems, necessary for its correct operation. The cooling system, on the top left side of Fig. 3, pumps deionized water from a reservoir and through the stack to regulate its temperature, dissipating the excess heat into the ambient air. On the left, the hydrogen supply circuit has a flow meter and a pressure regulator, to adjust the inlet pressure to 300 mbar before the hydrogen enters the stack. The power output system, at the bottom, allows for the regulated DC

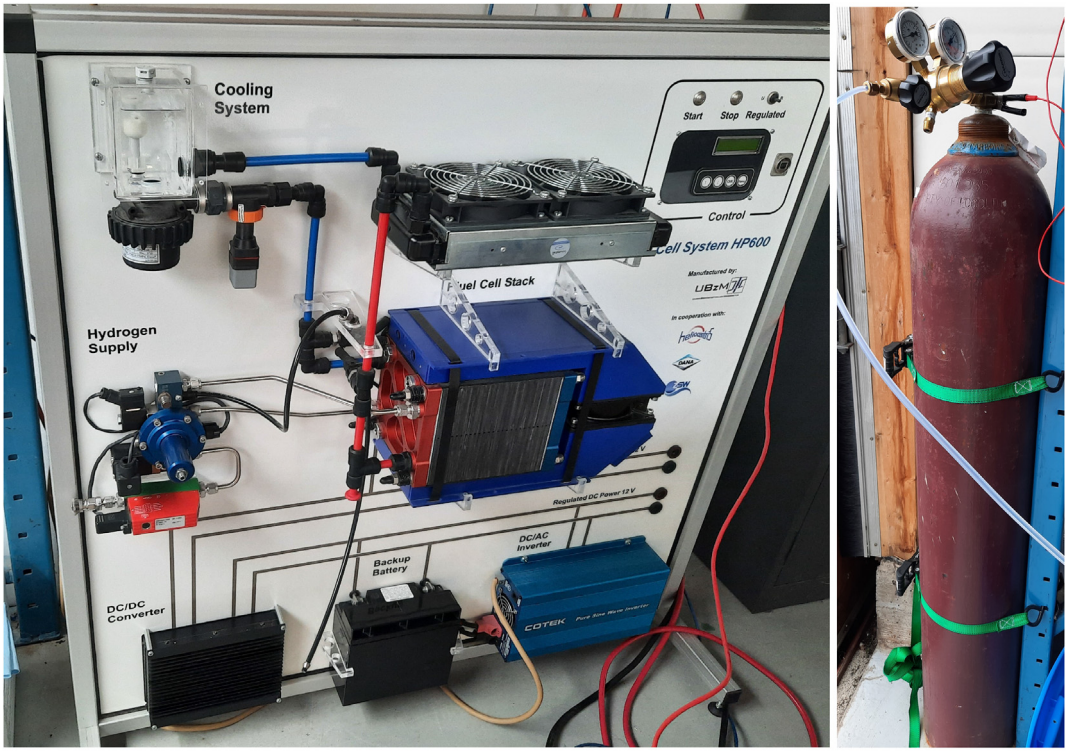

(a) HP 600 FC system.

(b) Hydrogen cylinder, with regulator.

Fig. 3 – FC system setup.

Please cite this article as: Farinha J et al., Hydrogen fuel cell integration and testing in a hybrid-electric propulsion rig, International Journal of Hydrogen Energy, https://doi.org/10.1016/j.ijhydene.2023.06.090

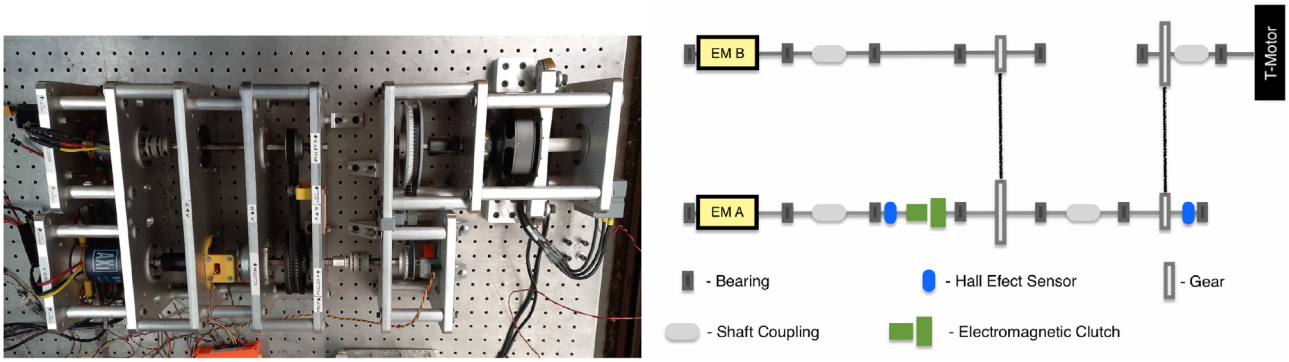

(a) Figure of the experimental apparatus.

(b) Diagram of the test bench, with the relevant elements highlighted.

Fig. 4 – The hybrid test bench.

(12 V) and AC (230 or 115 V) outputs of the system to function, by having, from left to right, a DC/DC converter, a backup battery, and a DC/AC inverter. Finally, at the top right corner there is the control panel, where the measured system variables can be read on an LCD screen, and the operating mode can be changed between regulated and unregulated.

Hybrid test bench

The hybrid test bench, portrayed in Fig. 4, is an experimental propulsion rig developed previously at the Centre for Aerospace Research (CfAR) [47–49], aiming to test hybrid propulsion solutions. It currently consists of a parallel configuration, schematized in Fig. 4 with a 4.2 kW AXI 5345/16 motor on the A side, and a 1.65 kW AXI 4130/20 on the B side. The output shaft is connected to a dynamometer – a 10 kW T-Motor U15II KV100 acting as a generator, whose three phase output is converted by a rectifier into DC current, which is then regulated and dissipated by a 5 kW electronic load.

Sensors

The test bench is equipped with different devices that allow for the data collection, namely:

- Two Hall Effect sensors to compute the rotational speed through the frequency of its square wave signal;
- Two current shunts to survey the current values in each side, by assessing the voltage drop across its small but very precise 250 μΩ resistance;
- Two voltage divider circuits, to step down the battery tension by a factor of 10.

All the data from the sensors is read by the appropriate National Instruments' cards, using the NI cDAQ-9188 chassis. It is then processed, displayed, and recorded by a LabVIEW program, developed specifically for this purpose.

Actuators

The actuators of the apparatus focus on the control of the testing conditions, being:

- The two Electronic Speed Controllers (ESC) - the Jeti Spin 125 Pro Opto on the A side, and the Velocity ESC by Currawong on the B side. The communication in each is conducted by Pulse Width Modulation (PWM) and Controller Area Network (CAN) bus protocols,[1] respectively;
- An electromagnetic clutch that allows to couple/decouple the sides of the test bench on command via a relay that is controllable by the user interface;
- An electronic variable load, that dissipates the current generated at the dynamometer setup [50], and is manually tunable, effectively allowing to adjust the desired counter-torque to be imposed at the dynamometer.

The control and monitoring of the test bench's actuators is also conducted through the same LabView Graphical User Interface (GUI).

Operating modes

The use of the clutch allows for the establishment of the basic four operating modes: *A only*, *B only*, *Dash/Hybrid* mode, and *Regeneration* mode. The two first comprise the isolated powering of the electric motor of each corresponding side. *Dash/Hybrid* mode is achieved by powering both sides simultaneously, producing the maximum output possible - this is the mode on which the FC testing described in this paper was performed. The *Regeneration* mode functions on the principle of powering a single motor/engine, while simultaneously absorbing current on the opposite motor (which acts as generator), with the intent of recharging the onboard batteries - this mode opens an interesting set of possibilities regarding power management strategies *in-flight*, but was not explored here, since the fuel cell system was not designed for external regeneration purposes, i.e., current should not be supplied to it.

Test procedure

The Fuel Cell System (FCS) was connected via the unregulated power output to the B side of test bench. The regulated power output - which provides a constant 12 V supply through the

[1] Although the communication is conducted via CAN bus for the Velocity ESC, the throttle command is still expressed as the pulse width of a PWM signal of corresponding throttle.

Please cite this article as: Farinha J et al., Hydrogen fuel cell integration and testing in a hybrid-electric propulsion rig, International Journal of Hydrogen Energy, https://doi.org/10.1016/j.ijhydene.2023.06.090

usage of an auxiliary battery - was not tested, due to incompatibility with the B side motor, that is designed to be powered by a 6 S–8S battery (24 V–32 V), and the corresponding ESC would not even activate at such low voltage. As such, the tests performed were knowingly non-optimal. For further testing on the test bench involving the fuel cell, a suitable motor must be implemented on the B side, and the gear ratios recalculated accordingly - i.e. rebuild the apparatus with emphasis on fuel cell integration.

To begin testing, the stack was first heated up to its operating temperature of 55 °C, by running it connected only to the electronic load, at 60% of its maximum power. Then, the fuel cell system could be connected to the hybrid test bench, while the electronic variable load was connected do the dynamometer system attached to the output shaft of the bench, effectively dissipating the power generated. The load imposed on the system was controlled by manually adjusting the desired current output at the T-Motor (as seen in Fig. 4b).

For each test, a full throttle sweep of the B side was performed, with 10% steps. For the A side, the throttle steps were of 10%, starting at 20% (there was no activation at 10%), and ending at 40%, to avoid overspinning the B side. Only *Dash* mode configurations were tested, since the fuel cell had already been characterized powering a single motor. The *Regeneration* mode was not explored, considering the FC does not work as energy storage akin to a battery, and connecting it to an external power input can damage the system. Each test was conducted once, and the test bench data was recorded at a rate of 20 Hz, while the stack variables had to be logged manually. The results presented below concern solely the steady state behaviour after stabilization in each step, with the uncertainties indicating the time variation present in each step.

Polarization curve

To set the benchmark performance of the FC stack, against which its behaviour could be compared during these hybrid tests, the current-voltage polarization curve had to first be determined. The nominal characteristics of the fuel cell stack are the ones summarized in section Fuel Cell System.

The test consisted in heating the stack to its operating temperature, as described above, and then, using the programmable load, setting the current of the stack to several values along its operating range, and measuring the corresponding stack voltage. This procedure was repeated three times, to confirm the reproducibility of the results, and the average performance was calculated.

The results of these experiments are presented in Fig. 5, which served as the reference for the comparison made in Section Stack Performance. The Exp. pol. curve avg. represents the average value of the experimental results, which was used as a reference against which the hybrid test data could be compared.

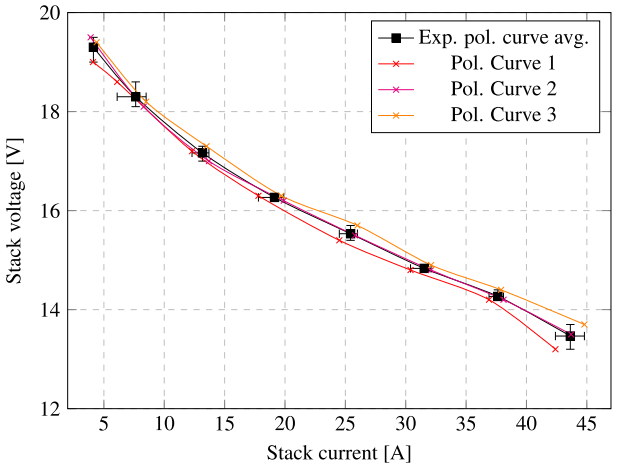

Fig. 5 – Fuel cell current-voltage polarization curve.

Results

Three different loads were tested: 0 A, 5 A, and 10 A. The plots in Fig. 6 show the measured variables for the tests performed with the 10 A load, and as a function of throttle B - represented as its PWM signal, which was digitally generated by the LabView software and transmitted to the ESC. The hybridization degree of the system was defined as the ratio between the power on the B side and the total power - on the premise that the fuel cell would be the lesser source of power in this configuration.

All the presented variables were affected by the throttle percentage of side A in predictable ways. With the increase in throttle, for either motor, there was an associated increase in the system's rotational speed (Fig. 6c), as more average voltage was being supplied to the Electric Motor (EM). This, in turn, came with an increase in the power consumed by each motor - Fig. 6a. For each side A throttle setting, however, the power being consumed decreased when the side B throttle was increased, since more of the power needs of the system were being met by the side B EM; this decrease reached 40.3%, for the 20% throttle A scenario, when the highest fuel cell power output during testing was reached: 257.8 W. This translates to an increase in the hybridization degree with the side B throttle, as seen in Fig. 6b, reaching 75.8% for the 20% throttle A scenario. Besides, the increase in the side B power was possible because the fuel cell current - Fig. 6d - was able to compensate the voltage drop (much larger than what was observed for lithium-polymer batteries in previous tests, which were no greater than 1 V) to keep up the power demand, in line with the fuel cell's polarization curve.

This FC is rated for up to 45 A, of which only around 19 A were used, as illustrated in Fig. 6d. Higher currents could likely have been reached if the load would have been taken further, but given the already severe undervoltage of the motor, this approach was not undertaken. Additionally, it can be seen in Fig. 6d as well that the fuel cell voltage was very steady after stabilizing in each step, with very little time variance, while in the case of the current this variation was slightly more noticeable.

The plots in Fig. 7 show the same variables, but now for the tests performed with the 5 A load. The overall system behaviour is the same as previously, but showing different values, given the reduced loading used. In particular, the power necessary to rotate the system decreases, for the same throttle settings - as shown in Fig. 7a - where the A side power

Please cite this article as: Farinha J et al., Hydrogen fuel cell integration and testing in a hybrid-electric propulsion rig, International Journal of Hydrogen Energy, https://doi.org/10.1016/j.ijhydene.2023.06.090

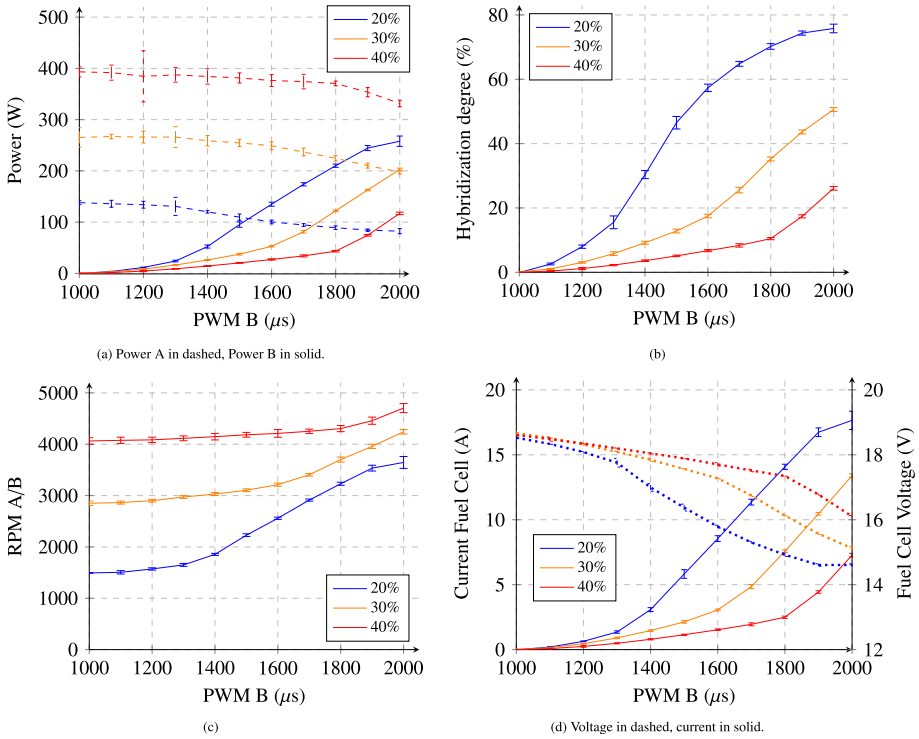

(a) Power A in dashed, Power B in solid.

(b)

(c)

(d) Voltage in dashed, current in solid.

Fig. 6 – Results for fuel cell power integration on the B side, with a 10 A load at the dynamometer, for different values of throttle A.

in the 20% throttle A scenario was mitigated in 47.46%, as more power demand was sustained by the fuel cell. For side B, this decrease in power comes from a significant decrease in the current being supplied to the motor (see Fig. 7d): for maximum B throttle and 20% A throttle the current is now just above 15 A, compared to about 19 A previously observed. Given the fuel cell performance, this comes with a smaller drop in the voltage.

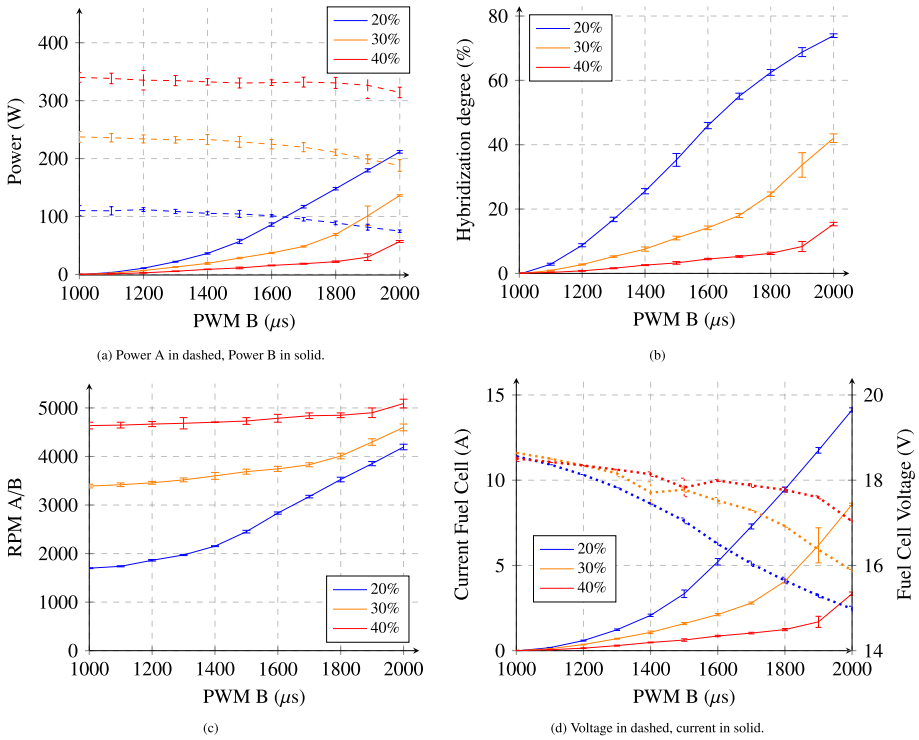

(a) Power A in dashed, Power B in solid.

(b)

(c)

(d) Voltage in dashed, current in solid.

Fig. 7 – Results for fuel cell power integration on the B side, with a 5 A load at the dynamometer, for different values of throttle A.

Please cite this article as: Farinha J et al., Hydrogen fuel cell integration and testing in a hybrid-electric propulsion rig, International Journal of Hydrogen Energy, https://doi.org/10.1016/j.ijhydene.2023.06.090

The smaller torque necessary to rotate the system also translated to an increase in the rotational speed of the whole system by several hundred RPM, as seen in Fig. 7c. Besides, with the increase in power demand, there was a smaller share of it being drawn from side B, leading to a noticeable decrease in the hybridization degree in Fig. 7b, for all throttle instances.

In the unloaded tests of Fig. 8, unlike what was done in the loaded tests, the side A throttle was not increased beyond 30%. This was because, for this throttle setting, the degree of hybridization was already quite low, only at around 30% (while it was nearly 50% with the 10 A load), as is shown in Fig. 8b Increasing the side A throttle even further would only reduce the overall influence of side B and would result in uninteresting results. Still, the general trend of the data, with the increments in both A and B throttle are in line with the loaded tests, as expected, with increases in rotational speed with both throttles (Fig. 8c), the decrease in B power with the larger throttle A (Fig. 8c), and the dropping of the fuel cell voltage with throttle B again accompanied by the contrasting increase in current (Fig. 8d).

The mismatching result obtained on the measurement of the motor's current at the 90% testing point of throttle B was revealed upon a closer inspection to derive from a particular system resonance affecting the B motor at this set of specific conditions, resulting in it drawing a fluctuating amount of current from the fuel cell. This was however a very contained phenomenon, quickly disappearing for either smaller or larger rotational speeds.

In these unloaded tests, as no electrical power was being generated by the dynamometer, all the power from sides A and B was being mechanically dissipated by the system. This corresponded mainly to the power necessary to overcome the rotational friction between components, and in a less significant way to the dissipated power in the coils of the two motors. Even in the loaded tests (Fig. 9b), this lost power represents a significant part of the total power supplied to the system, as evidenced by the plots in Fig. 9, which show the total electrical power the system receives, and the mechanical power generated at the output for both cases.

In both load scenarios the power input and mechanical output clearly increased with the throttle setting. It should be remarked however that even in the no load scenario (Fig. 9a), there is still mechanical power being consumed by the dynamometer – there being no current drawn from it, this is simply the result of its internal friction that applies a slim counter-torque to the system. Although the dynamometer power follows the trend of the total power input for all cases, a permanent gap is present, pointing out the transmission inefficiencies of the system, as well as the electric to mechanical power conversion by the motors - both at the input and at the dyno.

Stack performance

The fuel cell behaviour can also be analyzed and compared to previous observations. With that goal, the plot from Fig. 10 is included, which shows the FC's voltage and current for each test, in the order they were performed, alongside the experimental average described in section Polarization Curve.

Here, the most obvious aspect to notice is the considerably lower voltage observed in these hybrid tests, when compared to the polarization curve previously determined. Crucially, as mentioned in the test procedure description, for these experiments the programmable load was used for the hybrid test bench and could not be connected to the FC stack to warm it

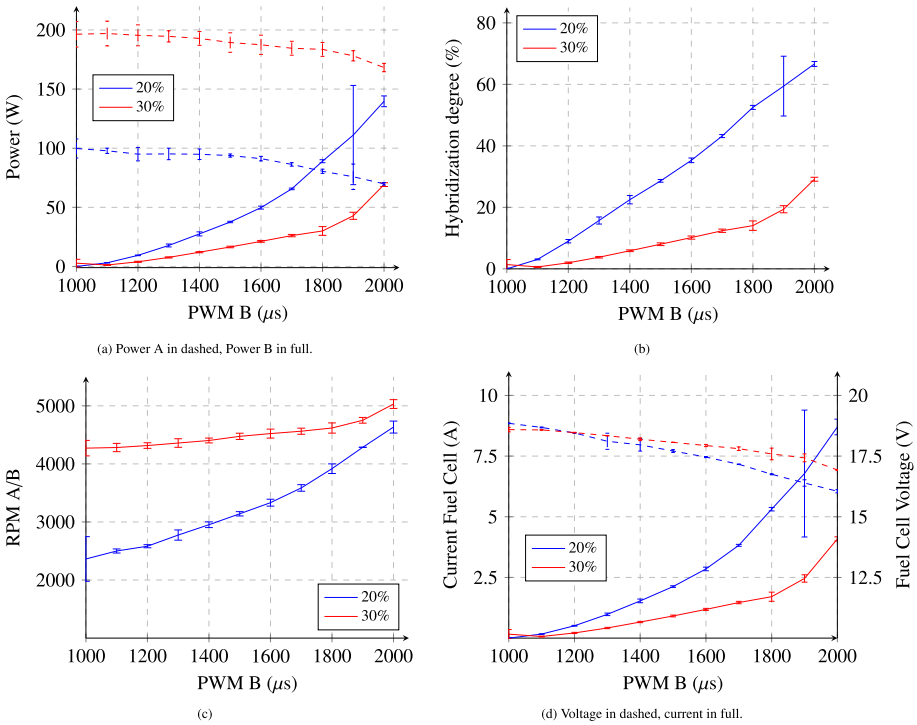

Fig. 8 – Results for FC power integration on the B side, with no load at the dynamometer, for different values of throttle A.

Please cite this article as: Farinha J et al., Hydrogen fuel cell integration and testing in a hybrid-electric propulsion rig, International Journal of Hydrogen Energy, https://doi.org/10.1016/j.ijhydene.2023.06.090

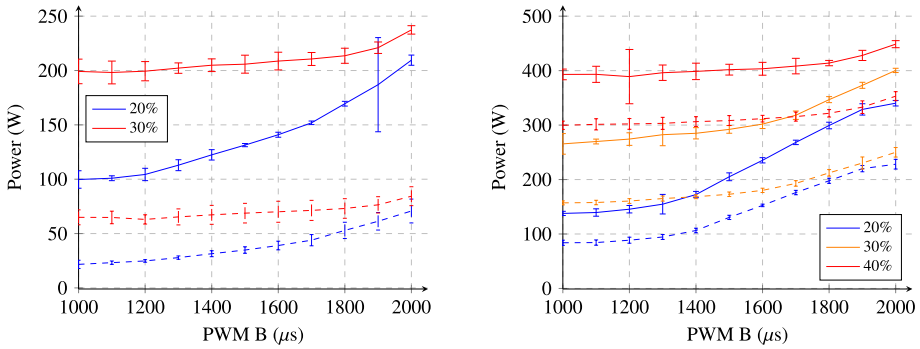

(a) Power A+B in solid, dynamometer power in dashed. No load applied.

(b) Power A+B in solid, dynamometer power in dash. Applied load of 10 A

Fig. 9 – Power values for FC integration on the B side, with and without load at the dynamometer, for different values of throttle A.

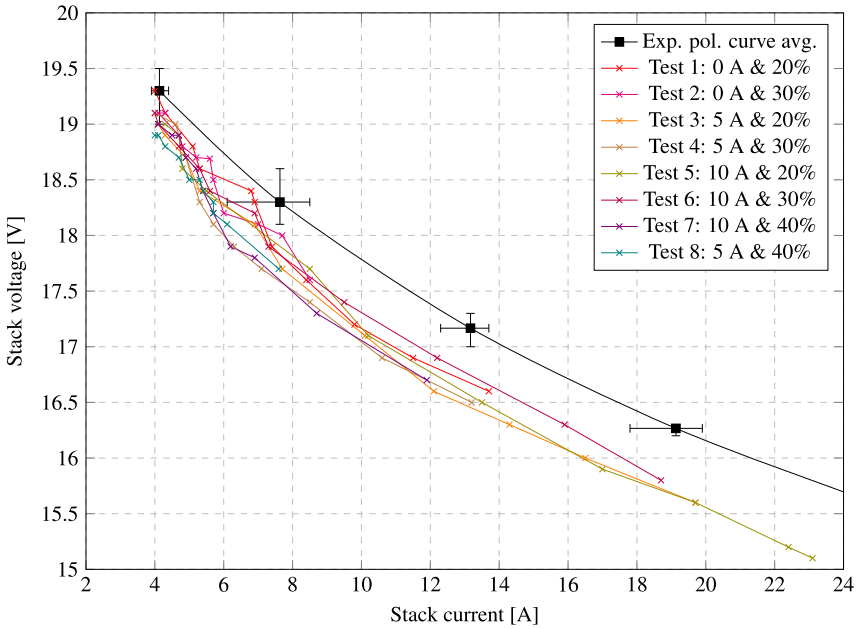

Fig. 10 – Fuel cell current-voltage behaviour during the hybrid tests.

up in-between tests. Therefore, given the relatively low current being drawn, the temperature of the stack steadily decreased throughout the tests. In fact, the first test was already performed at a temperature of 47.8 °C (instead of the 55 °C of previous tests), and only two tests could be run before the temperature of the FC stack dropped below the lower limit given by the manufacturer for operating temperature (45 °C). By the end of the eight tests, the temperature measured by the stack was as low as 40.6 °C. Therefore, due to limitations in the available equipment, it was not possible to perform these tests in the same starting conditions as the previous ones.

For the smallest current (at 0% throttle), for example, the first test showed a stack voltage of 19.3 V, in line with the previous average, but that value became smaller as the tests progressed, with only 18.9 V in the last one. The voltage difference between the curves also grows larger, as more current is being drawn, to about 0.8 V of difference for the largest current observed. While this may represent only about 5% of the total voltage of the FC, it is still a much higher variation in performance than what is observed when the fuel cell was operating consistently at the same temperature in previous tests. This indicates that, for a more stable fuel cell performance, a more advanced thermal management [42] system might be recommended, as the current system only has a cooling system to avoid overheating.

Conclusions

The power integration of the hydrogen FC functioned as a proof of concept for the employment of a hydrogen-powered electric motor in a parallel hybrid configuration.

As shown by the individual power evolution of both sides throughout the throttle sweeps, the fuel cell was able to significantly reduce the power drawn on the A side, without changing the system loading or the A side settings - for the highest load tested, the fuel cell was able to reduce the power being drawn on the opposite side of the hybrid configuration

Please cite this article as: Farinha J et al., Hydrogen fuel cell integration and testing in a hybrid-electric propulsion rig, International Journal of Hydrogen Energy, https://doi.org/10.1016/j.ijhydene.2023.06.090

by up to 40.3%, with a hybridization degree of 75.8%, presenting a maximum power output of 257.8 W. This dynamic power splitting shows promise in lessening fuel consumption in a possible hydrogen fuel cell – internal combustion engine configuration. Although the tests conducted were successful, the fuel cell's voltage capabilities are under sized for the motor to which its output was connected – this limitation did not allow to draw the total possible power from the fuel cell stack.

The stack also demonstrated a considerable dependency of its operating performance on the testing conditions, namely the temperature; the comparison with its benchmark experimental data revealed a distinguishable offset on the output current in the instance where the stack temperature was not according to the manufacturer's recommended value. For a better and more stable performance, a thermal management system more advanced than the one included in the fuel cell system would be necessary.

For future work, further test are planned using a test bench designed with fuel cell usage in mind, namely incorporating an electric motor with an adequate voltage constant, and tuning the gear ratio between sides accordingly. Nevertheless, these tests serve as small steps towards the implementation of a feasible aircraft hybrid propulsion system for aUAV.

Declaration of competing interest

The authors declare that they have no known competing financial interests or personal relationships that could have appeared to influence the work reported in this paper.

Acknowledgements

F.A. and A.S. acknowledge Fundação para a Ciência e a Tecnologia (FCT), through IDMEC, under LAETA, project UIDB/50022/2020. A.S. also acknowledges the NSERC Canada Research Chair funding program.

REFERENCES

[1] Lee D, Fahey D, Skowron A, Allen M, Burkhardt U, Chen Q, Doherty S, Freeman S, Forster P, Fuglestvedt J, Gettelman A, De León R, Lim L, Lund M, Millar R, Owen B, Penner J, Pitari G, Prather M, Sausen R, Wilcox L. The contribution of global aviation to anthropogenic climate forcing for 2000 to 2018. Atmos Environ 2021;244:117834. https://doi.org/10.1016/j.atmosenv.2020.117834.

[2] Penner JE, Lister DH, Griggs DJ, Dokken DJ, M M, editors. IPCC special report aviation and the global atmosphere - summary for policymakers. IPCC Secretariat; 1999.

[3] IPCC Working Group III. Climate change 2014 mitigation of climate change - working group III contribution to the fifth assessment report of the intergovernmental panel on climate change. Cambridge University Press; 2014.

[4] Penner JE, Lister DH, Griggs DJ, Dokken DJ, M M, editors. Aviation and the global atmosphere. Cambridge University Press; 1999.

[5] Grobler C, Wolfe PJ, Dasadhikari K, Dedoussi IC, Allroggen F, Speth RL, Eastham SD, Agarwal A, Staples MD, Sabnis J, Barrett SRH. Marginal climate and air quality costs of aviation emissions. Environ Res Lett 2019;14(11):114031. https://doi.org/10.1088/1748-9326/ab4942.

[6] Yim SHL, Lee GL, Lee IH, Allroggen F, Ashok A, Caiazzo F, Eastham SD, Malina R, Barrett SRH. Global, regional and local health impacts of civil aviation emissions. Environ Res Lett 2015;10(3):034001. https://doi.org/10.1088/1748-9326/10/3/034001.

[7] Brelje BJ, Martins JR. Electric, hybrid, and turboelectric fixed-wing aircraft: a review of concepts, models, and design approaches. Prog Aero Sci 2019;104:1–19. https://doi.org/10.1016/j.paerosci.2018.06.004.

[8] Sahoo S, Zhao X, Kyprianidis K. A review of concepts, benefits, and challenges for future electrical propulsion-based aircraft. Aerospace 2020;7(4):44. https://doi.org/10.3390/aerospace7040044.

[9] Xie Y, Savvarisal A, Tsourdos A, Zhang D, Gu J. Review of hybrid electric powered aircraft, its conceptual design and energy management methodologies. Chin J Aeronaut 2021;34(4):432–50. https://doi.org/10.1016/j.cja.2020.07.017.

[10] Chan CC, Chau KT, Chau KT. Modern electric vehicle technology. Oxford University Press; 2001.

[11] Jiao K, Xuan J, Du Q, Bao Z, Xie B, Wang B, Zhao Y, Fan L, Wang H, Hou Z, Huo S, Brandon NP, Yin Y, Guiver MD. Designing the next generation of proton-exchange membrane fuel cells. Nature 2021;595:361–9. https://doi.org/10.1038/s41586-021-03482-7.

[12] Rao AG, Yin F, Werij HG. Energy transition in aviation: the role of cryogenic fuels. Aerospace 2020;7(12):181. https://doi.org/10.3390/aerospace7120181.

[13] Baroutaji A, Wilberforce T, Ramadan M, Olabi AG. Comprehensive investigation on hydrogen and fuel cell technology in the aviation and aerospace sectors. Renew Sustain Energy Rev 2019;106:31–40. https://doi.org/10.1016/j.rser.2019.02.022.

[14] Acar C, Dincer I. The potential role of hydrogen as a sustainable transportation fuel to combat global warming. Int J Hydrogen Energy 2020;45(5):3396–406. https://doi.org/10.1016/j.ijhydene.2018.10.149.

[15] Faye O, Szpunar J, Eduok U. A critical review on the current technologies for the generation, storage, and transportation of hydrogen. Int J Hydrogen Energy 2022;47(29):13771–802. https://doi.org/10.1016/j.ijhydene.2022.02.112.

[16] Wang Y, Wu K, Zhao H, Li J, Sheng X, Yin Y, Du Q, Zu B, Han L, Jiao K. Degradation prediction of proton exchange membrane fuel cell stack using semi-empirical and data-driven methods. Energy and AI 2023;11:100205. https://doi.org/10.1016/j.egyai.2022.100205.

[17] De Lorenzo G, Agostino RG, Fragiacomo P. Dynamic electric simulation model of a proton exchange membrane electrolyzer system for hydrogen production. Energies 2022;15(17):6437. https://doi.org/10.3390/en15176437.

[18] Wang B, Zhao D, Li W, Wang Z, Huang Y, You Y, Becker S. Current technologies and challenges of applying fuel cell hybrid propulsion systems in unmanned aerial vehicles. Prog Aero Sci 2020;116:100620. https://doi.org/10.1016/j.paerosci.2020.100620.

[19] Bradley TH, Moffitt BA, Mavris DN, Parekh DE. Development and experimental characterization of a fuel cell powered aircraft. J Power Sources 2007;171(2):793–801. https://doi.org/10.1016/j.jpowsour.2007.06.215.

[20] Kim K, Kim T, Lee K, Kwon S. Fuel cell system with sodium borohydride as hydrogen source for unmanned aerial vehicles. J Power Sources 2011;196(21):9069–75. https://doi.org/10.1016/j.jpowsour.2011.01.038. fuel Cells Science & Technology 2010.

[21] Zhang X, Liu L, Dai Y, Lu T. Experimental investigation on the online fuzzy energy management of hybrid fuel cell/battery

power system for UAVs. Int J Hydrogen Energy 2018;43(21):10094–103. https://doi.org/10.1016/j.ijhydene.2018.04.075.
[22] Özbek E, Yalin G, Ekici S, Karakoc TH. Evaluation of design methodology, limitations, and iterations of a hydrogen fuelled hybrid fuel cell mini UAV. Energy 2020;213:118757. https://doi.org/10.1016/j.energy.2020.118757.
[23] Özbek E, Yalin G, Karaoglan MU, Ekici S, Colpan CO, Karakoc TH. Architecture design and performance analysis of a hybrid hydrogen fuel cell system for unmanned aerial vehicle. Int J Hydrogen Energy 2021;46(30):16453–64. https://doi.org/10.1016/j.ijhydene.2020.12.216.
[24] Liu H, Yao Y, Wang J, Qin Y, Li T. A control architecture to coordinate energy management with trajectory tracking control for fuel cell/battery hybrid unmanned aerial vehicles. Int J Hydrogen Energy 2022;47(34):15236–53. https://doi.org/10.1016/j.ijhydene.2022.03.036.
[25] Gong A, Palmer JL, Brian G, Harvey JR, Verstraete D. Performance of a hybrid, fuel-cell-based power system during simulated small unmanned aircraft missions. Int J Hydrogen Energy 2016;41(26):11418–26. https://doi.org/10.1016/j.ijhydene.2016.04.044.
[26] Gang BG, Kwon S. Design of an energy management technique for high endurance unmanned aerial vehicles powered by fuel and solar cell systems. Int J Hydrogen Energy 2018;43(20):9787–96. https://doi.org/10.1016/j.ijhydene.2018.04.049.
[27] Srinivasan S, Tiwari R, Krishnamoorthy M, Lalitha M, Raj K. Neural network based mppt control with reconfigured quadratic boost converter for fuel cell application. Int J Hydrogen Energy 2021;46(9):6709–19. https://doi.org/10.1016/j.ijhydene.2020.11.121.
[28] Y. Yan, B. Wang, C. Wang, D. Zhao, C. Xiao, Adaptive maximum power point tracking based on Kalman filter for hydrogen fuel cell in hybrid unmanned aerial vehicle applications, Int J Hydrogen Energy. doi:10.1016/j.ijhydene.2023.03.288.
[29] Ji Z, Qin J, Cheng K, Dang C, Zhang S, Dong P. Thermodynamic performance evaluation of a turbine-less jet engine integrated with solid oxide fuel cells for unmanned aerial vehicles. Appl Therm Eng 2019;160:114093. https://doi.org/10.1016/j.applthermaleng.2019.114093.
[30] Seyam S, Dincer I, Agelin-Chaab M. Investigation of two hybrid aircraft propulsion and powering systems using alternative fuels. Energy 2021;232:121037. https://doi.org/10.1016/j.energy.2021.121037.
[31] Farsi A, Rosen MA. Performance analysis of a hybrid aircraft propulsion system using solid oxide fuel cell, lithium ion battery and gas turbine. Appl Energy 2023;329:120280. https://doi.org/10.1016/j.apenergy.2022.120280.
[32] Giacoppo G, Barbera O, Briguglio N, Cipitì F, Ferraro M, Brunaccini G, Erdle E, Antonucci V. Thermal study of a SOFC system integration in a fuselage of a hybrid electric mini UAV. Int J Hydrogen Energy 2017;42(46):28022–33. https://doi.org/10.1016/j.ijhydene.2017.09.063.
[33] Rostami M, Manshadi MD, Farajollahi AH, Marefati M. Introducing and evaluation of a new propulsion system composed of solid oxide fuel cell and downstream cycles; usage in unmanned aerial vehicles. Int J Hydrogen Energy 2022;47(28):13693–709. https://doi.org/10.1016/j.ijhydene.2022.02.104.
[34] Gadalla M, Zafar S. Analysis of a hydrogen fuel cell-pv power system for small uav. Int J Hydrogen Energy 2016;41(15):6422–32. https://doi.org/10.1016/j.ijhydene.2016.02.129.
[35] Lapeña-Rey N, Blanco J, Ferreyra E, Lemus J, Pereira S, Serrot E. A fuel cell powered unmanned aerial vehicle for low altitude surveillance missions. Int J Hydrogen Energy 2017;42(10):6926–40. https://doi.org/10.1016/j.ijhydene.2017.01.137.
[36] Obertino D. Design and simulation study of a hybrid-electric propulsion system for a VTOL tilt-rotor UAV, master degree thesis. Politecnico Di Torino; December 2021.
[37] Pan Z, An L, Wen C. Recent advances in fuel cells based propulsion systems for unmanned aerial vehicles. Appl Energy 2019;240:473–85. https://doi.org/10.1016/j.apenergy.2019.02.079.
[38] González-Espasandín Óscar, Leo TJ, Raso MA, Navarro E. Direct methanol fuel cell (DMFC) and H2 proton exchange membrane fuel (PEMFC/H2) cell performance under atmospheric flight conditions of Unmanned Aerial Vehicles. Renew Energy 2019;130:762–73. https://doi.org/10.1016/j.renene.2018.06.105.
[39] Cheng X, Shi Z, Glass N, Zhang L, Zhang J, Song D, Liu Z-S, Wang H, Shen J. A review of PEM hydrogen fuel cell contamination: impacts, mechanisms, and mitigation. J Power Sources 2007;165(2):739–56. https://doi.org/10.1016/j.jpowsour.2006.12.012. iBA – HBC 2006.
[40] Gong A, Verstraete D. Fuel cell propulsion in small fixed-wing unmanned aerial vehicles: current status and research needs. Int J Hydrogen Energy 2017;42(33):21311–33. https://doi.org/10.1016/j.ijhydene.2017.06.148.
[41] Fernandes M, Andrade S de P, Bistritzki V, Fonseca R, Zacarias L, Gonçalves H, de Castro A, Domingues R, Matencio T. SOFC-APU systems for aircraft: a review. Int J Hydrogen Energy 2018;43(33):16311–33. https://doi.org/10.1016/j.ijhydene.2018.07.004.
[42] Xu J, Zhang C, Wan Z, Chen X, Chan SH, Tu Z. Progress and perspectives of integrated thermal management systems in pem fuel cell vehicles: a review. Renew Sustain Energy Rev 2022;155:111908. https://doi.org/10.1016/j.rser.2021.111908.
[43] Bose A, Zhu X. Design of stable and durable polymer electrolyte membrane fuel cells by embedding hydrophobic cage-structured material in cell components. Fuel 2019;235:954–61. https://doi.org/10.1016/j.fuel.2018.08.051.
[44] Barthelemy H, Weber M, Barbier F. Hydrogen storage: recent improvements and industrial perspectives. Int J Hydrogen Energy 2016;42(11):7254–62. https://doi.org/10.1016/j.ijhydene.2016.03.178. special issue on The 6th International Conference on Hydrogen Safety (ICHS 2015), 19-21 October 2015, Yokohama, Japan.
[45] Schömann J. Hybrid-electric propulsion systems for small unmanned aircraft, thesis. Technische Unisersität München; December 2013.
[46] Heliocentris Energy Systems GmbH. Operation guide - HP 600 fuel cell system. 3rd ed. January 2008.
[47] Machado L. Design and development of a hybrid electric propulsion system for unmanned aerial vehicles, master's thesis. Instituto Superior Técnico; May 2019.
[48] Matlock J. Evaluation of hybrid-electric propulsion systems for unmanned aerial vehicles, master's thesis. University of Victoria; 2019.
[49] Beagley A, Verhelst J, Schulz J, Frederiksen M, Giles M, Graham N. Mech 400 - design project. university of Victoria; April 2020.
[50] Brisebois C, Christison I, LeBlanc I, Perron R, Stacey J, Wilson J. Hybrid test bench dynamometer, mECH 400 capstone final report. University of Victoria; August 2021.

Please cite this article as: Farinha J et al., Hydrogen fuel cell integration and testing in a hybrid-electric propulsion rig, International Journal of Hydrogen Energy, https://doi.org/10.1016/j.ijhydene.2023.06.090